moves at a depth, it is to be expected that a signature of this would be available on the surface. It is observed from the results shown in Figure 2 *a–e* that the force centre location matches with the epicentre location. That this is not due to the geometry of the array is seen from Figure 2 *b* and *c* where the epicentre lies outside the area enclosed by the stations. Even in these cases the force centre is dispersed near the epicentre. Another interesting feature of the force centre is the direction of its movement. In Figure 2 *a* it is essentially in the E–W direction which matches with the direction of the major fault in the region with which the event is associated. The third interesting observation is that the maximum shift of the force centre correlates favourably with the length of fault rupture expected for the shock.

Admittedly there are several limitations in the arguments presented above. First of all, the effect of the vertical acceleration has not been included in the computations. The surface has been assumed to be planar which will not be valid, particularly in mountainous terrain. Three-dimensional nature of the medium and of the forces are yet to be considered in the analysis.

1. Amin, M. and Ang, A. H. S., *J. Eng. Mech. ASCE*, 1968, **94**, 559–583.
2. Iyengar, R. N. and Iyengar, K. T. S., *Bull. Seismol. Soc. Am.*, 1969, **59**, 1163–1188 .
3. Linsley, R. K., *Water Resources Engineering*, McGraw Hill Co, 1972.
4. Chandrashekharan, A. R. and Das, J., *Bull. ISET*, 1990, **27**, 1.

Received 3 October 1998; accepted 25 November 1998

Enigmatic orthopyroxene–rutile–spinel intergrowth in the mantle xenoliths from Kutch, India

N. R. Karmalkar*†§, R. A. Duraiswami*, W. L. Griffin†‡ and S. Y. O'Reilly†

*Department of Geology, University of Pune, Pune 411 007, India
†GEMOC Key Centre, Macquarie University, Sydney 2109, Australia
‡CSIRO Exploration and Mining, P.O. Box 136, North Ryde, NSW 2113, Australia

Several olivine nephelinite and alkali olivine basalt plugs intrude the flat lying gently dipping Mesozoic sediments of Kutch. Most of these plugs contain ultramafic xenoliths of mantle origin. The ultramafic xenoliths are mostly spinel-lherzolites with Cr-diopsides as the clinopyroxene phase. The orthopyroxenes in the spinel lherzolite from Mt. Sayala Devi contain numerous platelets of spinel. Besides the spinels, these also contain highly birefringent acicular inclusions with inclined extinction. Partial microprobe studies have identified the inclusions as rutile. The anomalous habit of the rutile indicates probable exsolution. On the basis of petrographic observations and the geochemical characteristics, the formation of such rutile has been discussed. Such intergrowths have been described previously as exsolution feature during cooling at high pressure. However, in the present instance it seems to be a low-pressure, low-temperature phenomenon with the onset of mantle metasomatism.

THE Peninsula of Kutch on the northwestern edge of the Deccan Volcanic Province is better known for its fossiliferous Mesozoic sediments. In Kutch, the Deccan basaltic flows are confined to a long strip bordering the sedimentary highlands from Lakhpat in the northwest to Anjar in the east[1]. The Mesozoic sediments of Kutch are intruded by a number of volcanic plugs and sheet-like bodies, most of which are present in the central and northern part of the mainland. While prominent plugs occur at Dhrubia, Sayala Devi, Vethon, Bharapar and Dinodhar Dongar, sheet-like bodies occur at Bhujia and Lodlai. The intrusions and sheets, unlike the thoeliite flows, are of olivine nephelinite and alkali olivine basalts. As the basaltic flows are confined to the southern and western part of the mainland and are absent in the central and northern parts, direct relation between the plugs and the basaltic flows is not seen. The alkaline intrusions are known to entrain ultramafic xenoliths of mantle origin[2,3].

For the present study more than thirty spinel lherzolite xenoliths from Mt. Sayala Devi were collected and cut into 5 mm slabs. Microscopic observations helped to identify the mineral phases and their textures. Modal abundance of minerals was determined by point counting of thin polished sections. The major element compositions were determined on polished thin sections using an automated CAMEBAX SC-50 electron microprobe at the Macquarie University, Australia, in wavelength dispersive analysis mode, with natural and synthetic mineral standards. A UV laser ablation microprobe coupled to an ICPMS was used to determine trace element concentrations at the same institute. Four representative xenoliths were selected for detailed chemical analysis on the basis of their size, freshness and petrological interest such as the presence of the rutile exsolutions of anamolous habit in the orthopyroxenes. The trace element and REE data for the clinopyroxenes are pre-

§For correspondence

sented in the form of spidergrams (Figure 1). The trace and REE values are normalized to the primitive mantle values (3 × chondrite values). The orthopyroxenes have low contents of REE, when compared to the concentrations in clinopyroxenes. The data are presented in the form of abbreviated spidergrams (Figure 2).

The mantle xenoliths from Mt. Sayala Devi are comparatively fresh and appear to be concentrated at the lower levels of the plug. They are granular and are oblong-elongated in shape, range in size between 1 and 2 cm, but xenoliths as large as 4–5 cm are also not uncommon. Petrographically, the xenoliths contain olivine, orthopyroxene (enstatite), clinopyroxene (Cr-diopside, Cr_2O_3: 0.67 to 1.16 wt%) and spinel. The xenoliths are devoid of any hydrous or volatile-bearing minerals such as amphibole, phlogophite and apatite. The xenoliths contain 31.2–79.4% olivine, 2.6–23.9% orthopyroxene, 0.0–8.4% clinopyroxene and 0.0–5.3% spinel. On the basis of the modal abundances of the mineral phase, some of these xenoliths can be best classified as spinel harzburgites[4], but are referred to here as lherzolite since the clinopyroxenes, although low in modal abundance, are saturated in calcium[5] (CaO: 22.34 to 23.98 wt%). Modal abundance (Table 1) of clinopyroxenes vary considerably, which is suggestive of varying degree of partial melting[5].

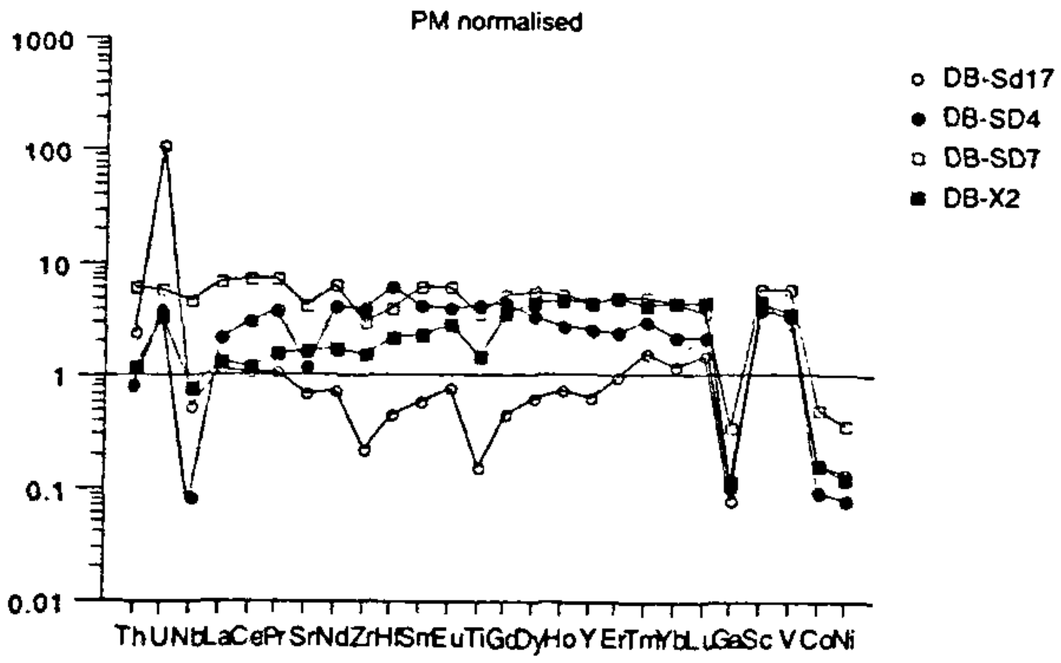

Figure 1. Spidergram of trace element and REE contents of clinopyroxenes, normalized to primitive mantle[36] (Th: 0.008, U: 0.024, Nb: 0.738, La: 0.704, Ce: 1.810, Pr: 0.267, Sr: 23.40, Nd: 1.357, Zr: 11.82, Hf: 0.312, Sm: 0.441, Eu: 0.168, Ti: 1308.0, Gd: 0.590, Dy: 0.728, Ho: 0.167, Y: 4.68, Er: 0.477, Tm: 0.073, Yb: 0.488, Lu: 0.073, Ga: 30.0, Sc: 17.46, V: 169.5, Co: 1506.0, Ni: 33000.0 ppm) in spinel lherzolite xenoliths from Mt. Sayala Devi, Kutch.

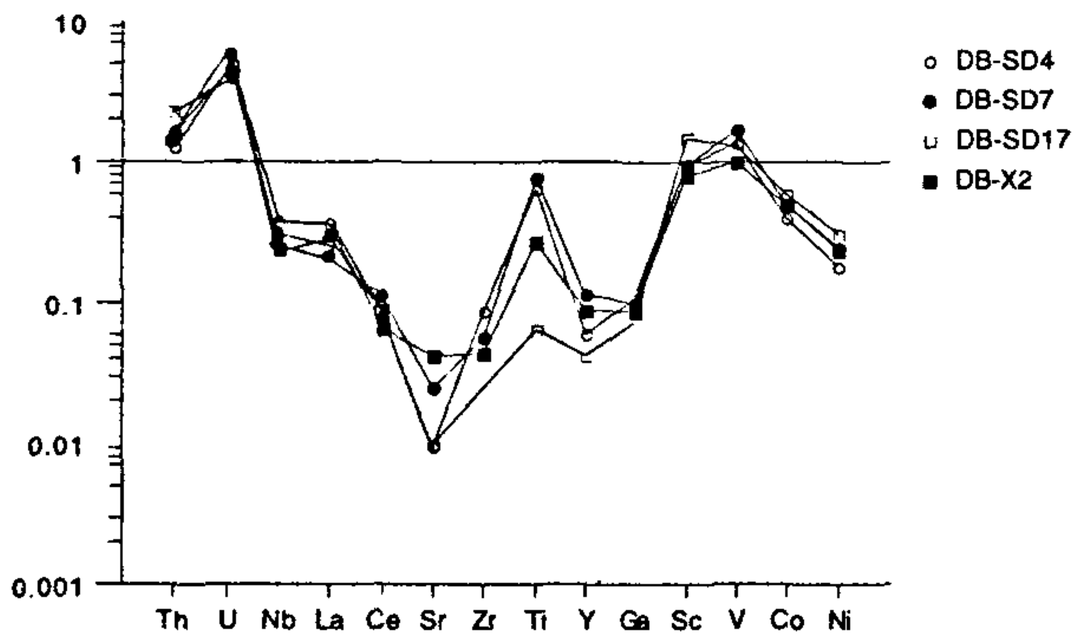

Figure 2. Abbreviated spidergrams of trace elements and REE contents in orthopyroxenes, normalized to primitive mantle[36], in spinel lherzolite xenoliths from Mt. Sayala Devi, Kutch.

The xenoliths exhibit porphyroclastic texture[6] or xenomorphic granular texture[7]. Weak foliation is discernible in few sections. On the basis of the composition of the clinopyroxenes, most xenoliths belong to type I, but a few also belong to type II (ref. 8). Olivine porphyroclasts (1–2 mm) are mildly strained and display strain shadows and kink bands which are characteristic features of the mantle peridotites[6]. Some of these olivine porphyroclasts are fractured and contain trails of fluid inclusions. The clinopyroxene is emerald green and occurs as small grains (0.5–1 mm) that are interstitial to olivine and orthopyroxene. Sometime they exhibit fine exsolution lamellae of orthopyroxene. Spinels occur as reddish-brown, subhedral grains. Although the spinels are present in close association with orthopyroxene and clinopyroxene, they do not show any symplectic intergrowth. Skeletal black spinels breaking down at the periphery into small, tiny, vermicular grains are common towards the edge of the xenoliths. Variable amounts of spongy green glass is seen interstitial to the other mineral phases or filling the vugs. The glass is enriched in silica, alumina and the alkalies (Table 2). Such glasses are considered as a product of volatile aided incongruent dissolution of clinopyroxenes during heating and decompression of the xenoliths[9]. Although no carbonate has been observed in the samples studied, such glasses have been interpreted as the product of reaction between mantle rocks and carbonate-rich fluids[10].

The orthopyroxenes from Mt. Salaya Devi are subhedral and occur as porphyroclasts (1–2 mm) and neoblasts (< 1 mm). The orthopyroxene porphyroclasts exhibit finely-spaced exsolution lamellae. The orthopyroxene in sample DB SD-1, DB SD-3, and DB SD-4 contain acicular, prismatic and highly birefringent inclusions (Figure 3). These needles show strong preferred orientation in two directions within the ortho-pyroxenes. Some of these cross each other at right angle. All needles in one set do not extinguish together, but over a range of extinction angles from zero to 33°. Similar features have been recorded[11] and are identified as anomalously elongated rutile[12]. In the present case, the rutile grains are not large enough to yield complete chemical analysis. Partial analysis of these inclusions is found to be rich in TiO_2 content. However, along with the rutile some portion of the accompanying orthopyroxenes is also getting analysed, which is evident

Table 1. Modal abundances of Mt. Sayala Devi xenoliths

	SD-1	SD-2	SD-3	SD-4	SD-5	SD-7	SD-11
Olivine	31.2	65.0	64.1	28.0	73.4	55.9	91.4
Orthopyroxene	20.5	25.2	18.7	23.9	3.0	7.7	2.6
Clinopyroxene	1.5	0.0	0.5	2.5	1.2	1.9	2.3
Spinel	4.9	2.7	1.1	5.3	3.1	5.1	0.0
Glass	41.7	6.8	15.6	40.0	19.1	29.2	3.7
Total	99.8	99.7	100.0	99.7	99.8	99.8	100.0

	SD/13A	SD-13/B	SD-13/C	SD-74/A	SD-74/B	SD-X2/A	SD-X2/B
Olivine	64.7	79.4	67.3	62.3	67.2	58.7	55.8
Orthopyroxene	7.4	6.5	7.1	18.9	20.4	7.0	9.8
Clinopyroxene	0.9	3.3	0.2	0.4	0.5	8.4	6.1
Spinel	2.9	2.9	3.0	1.4	0.9	5.1	4.8
Glass	23.8	5.1	22.1	17.0	11.7	20.5	24.1
Total	99.6	96.2	99.7	100.0	100.7	99.7	100.6

Table 2. Electron microprobe analysis of orthopyroxene, spinel, glass and partial analysis of rutile from Mt. Sayala Devi, Kutch

	Orthopyroxene						Rutile
	64		68	73	99		67
	Core	Rim	Core	Core	Core	Rim	
SiO_2	55.19	56.32	55.75	51.38	55.59	55.05	22.43
TiO_2	0.13	0.05	0.15	0.08	0.12	0.15	38.12
Al_2O_3	3.24	2.69	3.49	6.12	3.53	3.33	1.21
Cr_2O_3	0.36	0.32	0.42	0.89	0.40	0.30	0.45
FeO	6.96	6.77	6.80	7.01	6.85	6.64	18.96
MnO	0.14	0.17	0.10	0.08	0.13	0.19	0.21
MgO	33.72	33.94	34.00	32.55	33.88	33.77	23.37
CaO	0.25	0.26	0.32	0.22	0.23	0.23	0.23
Na_2O	0.01	0.03	0.03	0.02	0.01	0.02	0.02
K_2O	0.00	0.02	0.02	0.03	0/00	0/00	0/00
NiO	0.02	0.13	0.03	0.06	0.00	0.07	0.18
Total	100.04	100.71	101.11	98.44	100.72	99.75	105.18
Mg #	89.62	89.93	89.91	89.22	89.81	90.06	68.72

	Rutile					Spinel	Glass
	69	70	71	75	101	66	79
SiO_2	18.71	33.00	36.51	29.05	5.84	3.77	65.65
TiO_2	69.39	42.34	29.76	50.89	64.72	0.07	0.28
Al_2O_3	1.01	1.58	3.80	1.37	0.43	48.55	18.45
Cr_2O_3	0.49	0.17	0.74	0.33	0.47	13.35	0.06
FeO	2.27	4.19	4.43	3.67	14.42	11.89	0.32
MnO	0.05	0.12	0.06	0.15	0.14	0.00	0.02
MgO	13.50	21.77	22.56	19.88	9.98	20.61	0.00
CaO	0.11	0.23	2.21	0.24	0.69	0.00	0.03
Na_2O	0.00	0.00	0.62	0.01	0.06	0.01	6.07
K_2O	0.00	0.01	0.03	0.04	0.00	0.00	8.38
NiO	0.00	0.04	0.10	0.00	0.19	0.36	0.02
Total	105.54	103.44	100.80	105.63	96.95	98.60	99.27
Mg #	91.38	90.26	90.07	90.60	55.21	75.55	

from the presence of higher MgO and FeO contents (Table 2) in the analysis which are responsible for the high totals (exceeding 100%). The exsolution of brown platelets of spinel, that are crystallographically arranged are also observed in the same orthopyroxenes.

The ultramafic xenoliths from the Kutch area are interesting from the point of view that the alkaline rocks, within which the xenoliths are entrained, are geographically in proximity to the Deccan tholeiites. Although the alkaline rocks are no where seen in direct contact with Deccan tholeiites in the field, the available ^{40}Ar–^{39}Ar ages for alkali basalts range between 64 ± 0.6 and 67.7 ± 0.7 Ma (ref. 13). One of the alkali basalts from Dharam hill gives an age of 68 ± 2 Ma. Tholeiitic basalts from the Deccan trap outcrop in the same area have yielded an age of 66.8 ± 0.3 Ma (ref. 13). This overlap in the ages suggests a close temporal association between these two types of magmatism[14]. Their close genetic relationship is also documented in the Sr and Nd isotopic studies, suggesting a common source of similar isotopic composition[14]. Thus the Kutch alkaline volcanics are spatially and temporally correlated with the Deccan basalts. In light of this, the overlap in the ages between the two types of magmatism is of great significance and the alkaline magmatism must have slightly preceded the tholeiitic activity[15]. This is in concurrence with the rapid northward movement of the Indian plate at the time of Deccan volcanicity. Occurrence of alkaline magmatism preceding the tholeiitic activity seems to be common to the areas of continental flood basaltic activity worldover. In the Siberian traps, lamprophyric magmatism appears to have both preceded and post-dated the basaltic eruption[16]. In the Karoo area of South Africa, alkaline igneous rocks were emplaced at the margin of the craton[17].

It is of interest to note that eruptions of continental flood basalts are widely attributed to plume activity of mantle. The Deccan flood basalt has been linked to the Reunion plume whose remaining tail is at present responsible for the alkaline activity on Reunion island in the Indian ocean[18–20]. All current models[21] of plate reconstruction indicate that as the Indian subcontinent drifted northward subsequent to the break up of Gondwanaland, its western margin passed over the Reunion hotspot at around 65 to 68 Ma. Plate reconstructions indicate that at about 65 Ma the Kutch–Kathiawar–Saurashtra province was close to or directly sitting over the hot spot[21]. We therefore strongly believe that the ultramafic xenoliths of mantle origin entrained in the alkaline rocks of the Kutch region are the samples of plume-affected mantle, i.e. Reunion plume.

The Mt. Sayala Devi plug is different from the other alkaline plugs in the Kutch region. The xenoliths encountered in this plug are large in size (4–5 cm) compared to the small sized (1–2 cm) xenoliths in other localities. The xenoliths here are of two types (Cr-diopside, Al augite)[8]. Besides, the REE signatures of

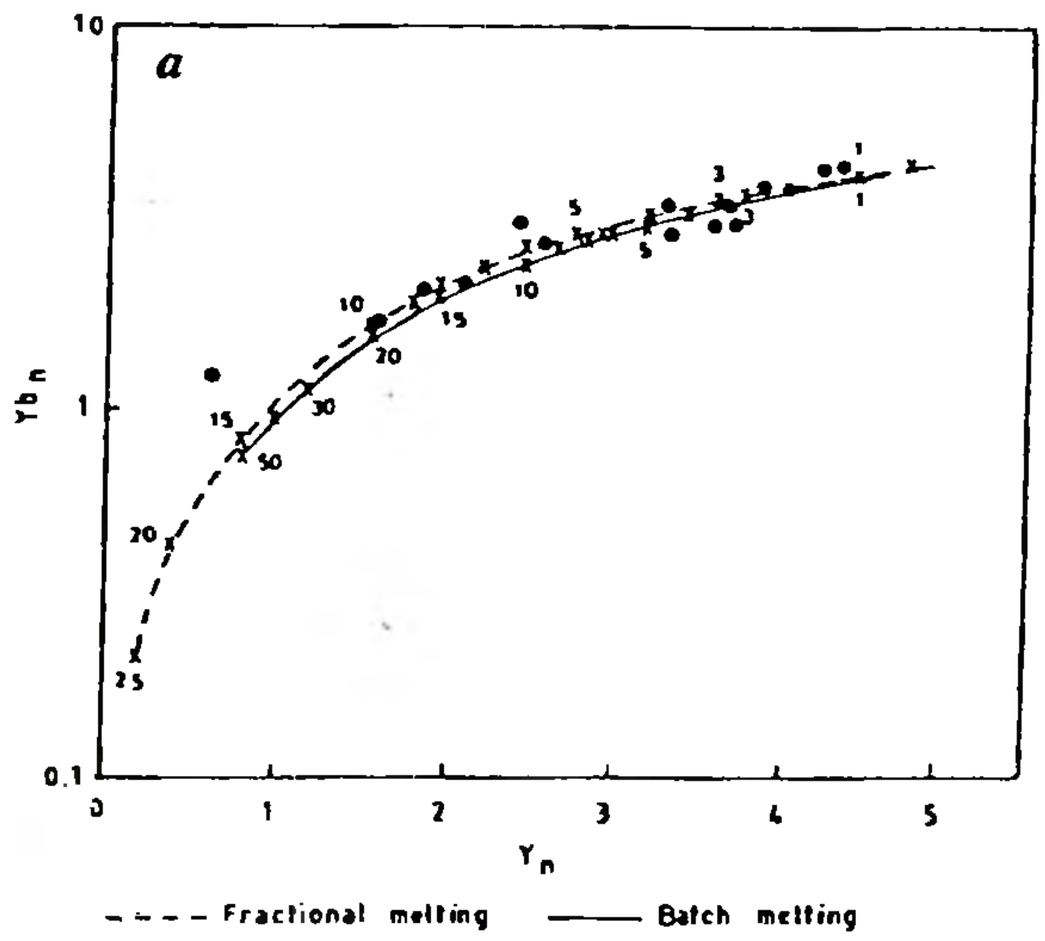

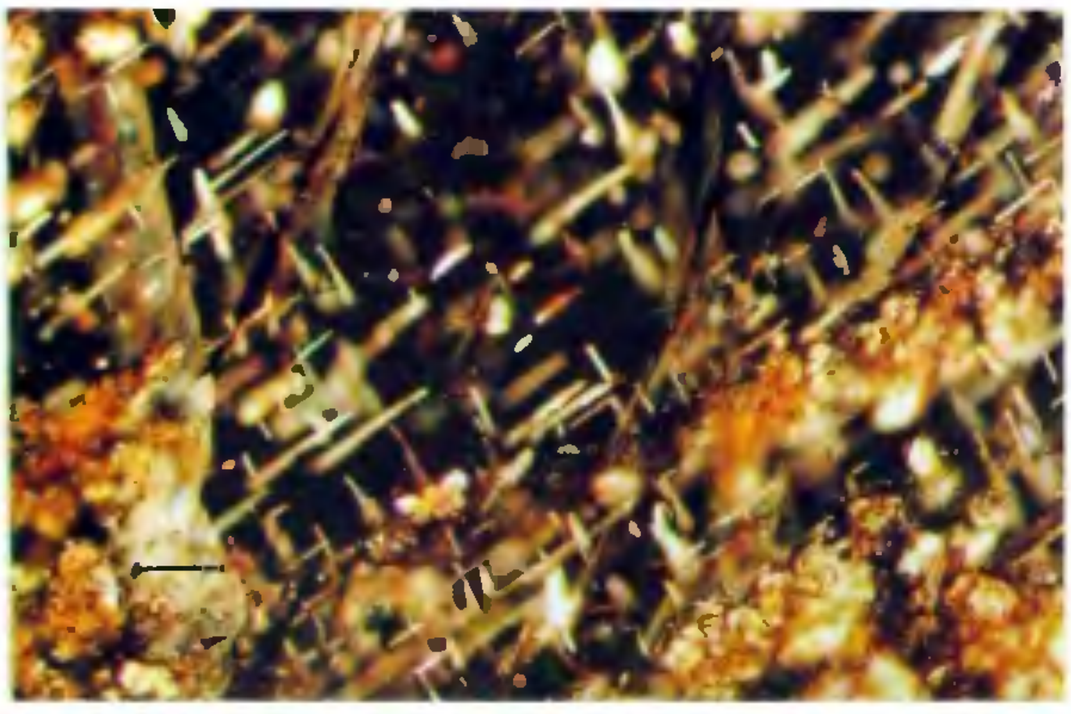

Figure 3. Photomicrograph of spinel lherzolite between cross nicols showing exsolution of acicular rutile in orthopyroxene (1 cm = 1 μm).

Figure 4. Melting models with (*a*), Y vs Yb and (*b*), Y vs Ti/Ti concentrations of clinopyroxenes from Mt. Sayala Devi, Kutch. The subscript *n* indicates that the elemental concentrations have been normalized to primitive mantle compositions[36].

these xenoliths are much different from those of the other plugs. The REE in the clinopyroxene of these samples (Figure 1) exhibit a relatively flat pattern without any significant enrichment in the LREE. In contrast, the REE in the orthopyroxenes exhibit depleted pattern (Figure 2). Trace element patterns of clinopyroxenes have been used to model melting conditions as has been done in the Mt. Shadwell xenoliths from Australia[5], which are petrographically and chemically similar to the Kutch xenoliths. The Y and Yb concentrations for the Kutch diopsides follow the predicted melting trends (Figure 4 *a*), with concentrations consistent to fractional and batch melting in the spinel peridotite field. In the fertile Kutch xenoliths the concentrations of the more compatible lithophile elements, such as Y and Yb, can be produced by 2 to 5% melting of a primitive mantle source, and for this small degree of melting the Y and HREE concentrations are insensitive to the style of melting (i.e. batch or fractional). The highly/more depleted samples would require about 45 to 50 degrees of batch melting (an unrealistically high value), but would require only 14 to 15% of fractional melting. The Sayala Devi xenoliths suggest both high (14 to 15% for DB SD-17) and low degrees of partial melting (2 to 5% for DB SD-4, DB SD-7 and DB SD-X2). This is also evident from the modal abundance of the clinopyroxene in the xenoliths, those with high amount of partial melting show low modal percentage of the clinopyroxene, while the others with low amount of partial melting have higher modal clinopyroxene. Hence the Sayala Devi xenoliths are most fertile and least metasomatized mantle samples in comparison to other xenolith localities in Kutch. The REE pattern of clinopyroxene, in the most depleted samples, viz. DB SD-17, exhibits low HREE, middle REE and LREE, excepting U and Th which show moderate enrichment. In contrast, the remaining samples display relatively flat to moderately enriched trend for the LREE. The clinopyroxene in all the samples exhibit a moderate to deep negative Ti and Nb anomalies and smaller Zr and Sr anomalies. The negative Ti–Nb–Zr anomalies can be explained partly as the product of partial melting by modeling the REE data (e.g. Figure 4 *b*). Interestingly, the accompanying orthopyroxenes exhibits small positive Ti anomalies (Figure 2), consistent with the petrographic observation of rutile exsolution/inclusions in at least a few samples. However, the observed positive Ti anomalies in orthopyroxene are not sufficient enough to balance the strong negative Ti anomalies in clinopyroxene. Thus the contention that the orthopyroxene can be significant carriers of Ti and the negative Ti anomaly in clinopyroxene are simply due to partitioning of Ti between clinopyroxene and orthopyroxene[22,23] does not hold good in the present case.

A small negative Zr anomaly is also characteristic of mantle clinopyroxenes[24,25]. These anomalies can be partly attributed to the process of partial melting, using appropriate distribution coefficients. The Ti and Zr concentrations in most samples broadly follow the concentrations expected from the melting model, provided the value of the distribution coefficient for Ti is slightly changed from 0.35 (ref. 5) to 0.1 in the initial compositions.

It has been observed by modeling the REE data that majority of the HREE can be produced by low degrees of partial melting, the moderately enriched nature of the LREE and MREE in some samples (DB SD-4 and DB SD-7) relative to the most depleted sample (DB SD-17) is in contrast to the one expected in residues of partial melting. Similarly, the depletion in the Ti, Nb, and Zr in clinopyroxene cannot be explained by partitioning these elements into co-existing Ti-bearing phases, excepting a possible rutile exsolution as observed in some of the orthopyroxenes. The worldwide occurrence of volatile-, silica-, and K-rich small melt fractions trapped in silicate mineral of basalt-borne xenoliths have been recently demonstrated[26]. Because of their silica- and volatile-rich compositions, these melts may be saturated in titanium oxides even for relatively low concentrations of Ti[27,28]. This characteristic is confirmed by the frequent occurrence of rutile and ilmenite among the 'daughter' minerals present as inclusions. Hence the melts identified in these inclusions represent very likely metasomatic agents for the spinel reaction rims. The rutile exsolution in the orthopyroxene are thus the products of such cryptic K-metasomatism. It has been already mentioned that the hydrous mineral phases such as amphibole, phlogopite and apatite are absent in the xenoliths studied. Spongy glass, which represents such melt fractions in the present instance, are also rich in silica and alkalies. Occurrence of such volatile-rich melt inclusions and small titanium oxide fractions in mantle xenoliths is consistent with continuous infiltration of small melt fractions in the lithospheric mantle, as has been proposed[29]. We therefore believe that the rutile inclusions in the orthopyroxenes from Sayala Devi mark the onset of mantle metasomatism. Besides rutile inclusion, the observed platelets of brown spinel in the orthopyroxenes appear to have been derived from the instability of Al during the introduction of metasomatic melt[30]. The strong correlation between the Al_2O_3 of the spinel and that of orthopyroxene and clinopyroxene suggest an underlying control over the composition of the accompanying spinel and partitioning of Al between clinopyroxene and orthopyroxene.

Pervasive interaction of the xenoliths with fluids rich in LREE is envisaged. The individual mineral grains in all the sample analysed are unzoned with respect to trace elements and hence the enrichment is an upper mantle event and not linked to recent alteration by the host basalt[31]. The metasomatic agent has influenced the

diffusion kinetics of the xenoliths during a cooling event. Such a diapiric upwelling of the plume-affected mantle would be in keeping with the evidence of the observed low equilibration temperatures (876–935°C), using Cr–Al–Orthopyroxene geothermometer[32] as well as the presence of exsolution lamellae in some of the diopsides. This implies that the fluid interacted at relatively low temperatures with the lithospheric mantle[31].

Similar occurrences of rutile as an exsolution/inclusion feature have been reported from the eclogite xenoliths in the kimberlite pipes of South Africa[12,33]. The present occurrence is different from the above reports in that the rutile in the present instance occurs within the orthopyroxenes, unlike those found in the clinopyroxene and garnet mineral phases, indicating cooling at low pressure as is evident by the absence of garnet in the xenoliths. Referring to the observed low temperatures in the present case to typical geotherms for areas of alkali basalt volcanism, such as the one derived for the Tertiary volcanism of south-eastern Australia[34], yields low pressure estimates of 9–12 kb, indicating entrainment of these lherzolite from relatively shallow depths (probably ≤ 35 km). These values are consistant with the estimated depth to the crust–mantle boundary (35–40 km) beneath Kutch, derived on the basis of modelling of the gravity data[35].

1. Biswas, S. K. and Deshpande, S. V., *J. Geol. Soc. India*, 1973, **14**, 134–141.
2. De, A., Report of 22nd Session of International Geological Congress, New Delhi, Part III, 1964, pp. 126–138.
3. Krishnamurthy, P., Pande, K., Gopalan, K. and Macdougall, J. D., *Geol. Soc. India Spl. Publ.*, 1989, **10**, 53–68.
4. Strickeisen, A., *Earth. Sci. Rev.*, 1976, **12**, 1–33.
5. Norman, M. D., *Contrib. Mineral. Petrol.*, 1998 (in press).
6. Mercier, J. C. and Nicolas, A., *J. Petrol.*, 1975, **16**, 454–487.
7. Harte, B., *J. Geol.*, 1977, **85**, 279–288.
8. Frey, F. A. and Prinz, M., *Earth Planet. Sci. Lett.*, 1978, **38**, 129–176.
9. Hauri, E. H., Schimizu, N., Dieu, J. J. and Hart, S. R., *Nature*, 1993, **365**, 221–227.
10. Ionov, D. A., Hofmann, A. W. and Shimizu, N., *J. Petrol.*, 1994, **35**, 753–785.
11. Moore, A. C., *Contrib. Mineral. Petrol.*, 1968, **17**, 233–236.
12. Griffin, W. L., Jensen, B. B. and Mishra, S. N., *Norsk Geologisk Tidsskrift*, 1971, **51**, 177–185.
13. Venkatesan, T. R., Pande, K. and Gopalan, K., *J. Geol. Soc. India*, 1986, **27**, 102–109.
14. Pande, K., Venkatesan, T. R., Gopalan, K., Krishnamurthy, P. and Macdougall, J. D., *Geol. Soc. India Spl. Publ.*, 1989, **10**, 145–150.
15. Karmalkar, N. R., Griffin, W. L. and O'Reilly, S. Y., 1998 (in preparation).
16. Lightfoot, P. C., Naldrett, A. J., Gorbachv, N. S., Doherty, W. and Fedorenko, V. A., *Contrib. Mineral. Petol.*, 1990, **104**, 631–644.
17. Kent, R. W., Storey, M. and Saunders, A. D., *Geology*, 1992, **20**, 891–894.
18. Duncan, R. A., *Tectonophysics*, 1981, **74**, 29–42.
19. Morgan, W. J., in *The Sea* (ed. Emiliani, C.), Wiley, New York, 1981, vol. 7, pp. 443–487.
20. Campbell, I. H. and Griffiths, R. W., *Earth Planet. Sci. Lett.*, 1990, **99**, 79–93.
21. Norton, I. O. and Sclater, J. G., *J. Geophys. Res.*, 1979, **84**, 6803–6830.
22. Rampone, E., Bottazzi, P. and Ottolini, L., *Nature*, 1991, **354**, 518–520.
23. McDonough, W. F., Stosch, H. G. and Ware, N. G., *Contrib. Mineral Petrol.*, 1992, **110**, 321–328..
24. Johnson, K. T. M., Dick, H. B. and Shimizu, N., *J. Geophys. Res.*, 1990, **95**, 2661–2678.
25. Ionov, D. A., Prikhodko, V. S. and O'Reilly, S. Y., *Chemical Geol.*, 1995, **120**, 275–294.
26. Scinao, P. and Clocchiatti, R., *Nature*, 1994, **368**, 621–624.
27. Ryerson, F. J. and Watson, E. B., *Earth Planet. Sci. Lett.*, 1987, **86**, 225–239.
28. Foley, S. F. and Wheller, G. E., *Chem. Geol.*, 1990, **85**, 1–18.
29. McKenzie, D., *Earth Planet. Sci. Lett.*, 1989, **95**, 53–72.
30. Haggerty, S. E., *Rev. Mineral.*, 1991, **25**, 184–185.
31. Witt-Eickschen, G. and Kramm, U., *J. Petrol.*, 1997, **38**, 479–493.
32. Witt-Eickschen, G. and Seck, H. A., *Contrib. Mineral. Petrol.*, 1991, **106**, 431–439.
33. Nixon, F. H., Knorring, O. von. and Rooke, J. N., *Am. Minerologist*, 1963, **48**, 1090–1132.
34. O'Reilly, S. Y. and Griffin, W. L., *Tectonophysics*, 1985, **111**, 41–63.
35. Raval, U. and Veeraswamy, K., in *Deccan Basalt* (eds Deshmukh, S. S. and Nair, K. K. K.), Gondawana Geol. Mag., 1996, spl. vol. 2, pp. 393–404.
36. Hofmann, A. W., *Earth Planet. Sci. Lett.*, 1988, **90**, 297–314.

ACKNOWLEDGEMENTS. N.R.K. thanks the Head of the Department of Geology, University of Pune, Pune, for granting special permission to collaborate with GEMOC Macquarie University, Sydney, Australia. R.A.D. is grateful to CSIR, New Delhi, for financial support in the form of SRF. We are also grateful to Miss Carol Lawson, Dr Norm Pearson for their help in the microprobe analysis and Mrs Ashwini Sharma for her help in the ICPMS microprobe analysis. We thank Dr Mark Norman and the post-doctoral fellows at the Centre for fruitful discussions.

Received 5 August 1998; revised accepted 14 December 1998